

IDENTIFICATION OF BURIED FAULTS IN EMBAYMENT AREA OF THE NORTHERN KHUZESTAN USING SEISMIC IMAGING

***Behnaz Nazmazar¹ and Mehdi Zare²**

¹*Department of Science, North Tehran Branch, Islamic Azad University, Tehran, Iran*

²*International Institute of Earthquake Engineering and Seismology, Tehran, Iran*

**Author for Correspondence*

ABSTRACT

This paper aims to identify the buried faults in the employment area of the northern Khuzestan using seismic-reflection data. This studied region is located in the southwest of central Iran, in the vicinity of Uromia Dokhtar region. Investigation of geological maps indicated that the region did not have any visible fault due to the thick alluvial cover. Interpretation of reflection data indicated that many faults existed in the region. In the northeastern part of the region, the majority of identified faults had a reverse mechanism with SW slope. In the southwestern part, some faults had normal mechanism with NE slope. Given the NW-SE trend of the identified faults, the lineament of the region, which is perpendicular to the faults, is likely to have had a significant role in the changed trend and the movement of the identified faults.

Keywords: *Embayment Area of the Northern Khuzestan, Seismic-Reflection Data, Buried Faults*

INTRODUCTION

Pazanan anticline is located in Zagros fold and thrust belt [embayment area of the northern Khuzestan]. This anticline has undergone a large number of fractures due to tectonic activities of the Zagros's dominant fold. Generally, the deformation of Zagros fold and thrust belt is the result of convergence between Arabic and Eurasian plates from middle-upper Cretaceous (Mann *et al.*, 2003). Neotethys has closed in the lower Miocene (Abdollahie Fard *et al.*, 2006) and Zagros fold and thrust belt has formed during the main orogenic phase of Zagros in the upper Miocene (Mann *et al.*, 1999).

Like other fold and thrust belts, the deformation of sediments in Zagros fold and thrust belt is due to the extension of detached thrusts parallel to orogenic trend and the accompanying folds. In contrast to the majority of such belts, however, the thrust faults tend to be hidden rather than being visible on the surface (Molinario *et al.*, 2005). These deformations have begun from the southern parts of Sanandaj-Sirjan belt following the continental contact between the Arabic plate and central Iran. The deformations have developed towards the foreland and are still developing (20 mm per year) (Tatar *et al.*, 2002). Pazanan anticline which is one of the biggest oil fields in the southwest of Iran has a NW-SE trend and its length and width are 60 km and 4-6 km respectively.

Like other Zagros structures, Pazanan anticline has a NW-SE trend. The central trend is N304 in the northwestern part and then reaches N328 with a rotation. Then, it comes back to the primary trend in the central parts and finally becomes N290 in the southeastern part. The maximum slope is 24-28 degrees in the northeastern ridge and 35-40 degrees in the southwestern ridge. The folded structures in Zagros mainly have parallel folds developed by bending mechanism of Cambrian rock units until Miocene (Tygel *et al.*, 1997).

Detachment fold is another type of folds in fold and thrust belts. These folds have a relatively stable rock layer and another layer with lower stability. In detachment folds, deformation is identified from the detachment surface (Shepherd, 1963; Stocklin, 1968; Falcon, 1969).

Detachment folds are formed where thrust platform is locked in a point and thrust movement reaches zero, preventing the fault from extending horizontally or with low angle. If this is the case, movement occurs in hanging wall parallel to fold and vertical lift occurs in the fault hanging wall (Berberian and King, 1981).

There are many detachment surfaces in Zagros belt during various stages of deformation, which have given rise to the geometrical complexity of the folds (Stoneley, 1981). In the studied region, the formations of *Harmoz*, *Sargelou*, *Goutina*, *Gerou*, *Kazhdomi*, *Gourpey*, *Pabdeh* and *Gachsaran* are considered as important detachment surfaces. Moreover, the steep front ridges have caused the development of fault

Research Article

extension folds in front of hidden thrusts of Zagros (Dahlstrom, 1990) and back thrust structures (Motiei, 1993) and out-of-sequence thrusts (Berberian, 1995) can be seen in some parts of the embayment anticline in the northern Khuzestan. Given the geometrical changes and structural style of Zagros fold and thrust belt, we measured the shortening rate in different sections of Zagros using various methods. According to GPS measurements in central Zagros, the current shortening rate is 10 mm per year in NNE-SSW direction, which constitutes around 50% of total convergence between Arabia and Eurasia (21 mm per year) (Motiei, 1995). A simple transverse profile of the folded Zagros (Poblet and McClay, 1996) indicated a shortened amount of 49 km, a balanced transverse cross-section of the southeastern part of Zagros (Vita-Finzi, 2001) indicates a shortened amount of at least 45 km [22%], and three transverse cross-sections of Fars, northern Khuzestan and Lorestan (Mitra, 2002) indicated a shortened amount of 70±20 km. This paper aims to identify the buried faults in the employment area of the northern Khuzestan using seismic-reflection data. The studied region is located in the southwest of Iran, in the vicinity of Uromia Dokhtar region.

MATERIALS AND METHODS

Research Method

Principles of CRS Method

CRS method is based on the features of reflective surface. Let's consider point R on the reflector. If we place a spring in point R , a spherical wave front with radius R_{NIP} will be produced. If we consider some part of reflective surface as a spring, a flat wave front with radius R_N will be produced. The idea of hypothetical wave front on reflective surface has been coined by Hubral (Mann *et al.*, 1999; Tygel *et al.*, 1997). Assuming that the ray is vertical, wave fronts contact the ground surface with angle α . Radius R_N , represents the reflector curvature, radius R_{NIP} represents the depth and angle of the same angle of reflective surface (Mitra, 2002).

$$t^2(x_m, h) = \left[t_0 + \frac{2\sin\alpha}{V_0} (x_m - x_0) \right]^2 + \frac{2t_0 \cdot \cos^2\alpha}{V_0} \left[\frac{(x_m - x_0)^2}{R_N} + \frac{h^2}{R_{NIP}} \right] \quad [1]$$

2D operator of CRS stacking, as shown in equation 1, is a hyperbolic estimation of the time (Blanc *et al.*, 1978) and shows the time of reflected rays in the vicinity of the ray.

Where, h is half of the offset between spring and receiver, x_m is the middle point between spring and receiver, and V_0 is the velocity of the surface layer.

For each sample $[t_0, x_0]$ in stack cross-section, seismic attributes including (α, R_N, R_{NIP}) must be determined. A method for determining the parameters is to intersect stacking operator with common middle record plate ($x_m = x_0$):

$$t_{CMP}^2(h) = t_0^2 + \frac{2t_0 \cdot h^2 \cdot \cos^2\alpha}{V_0 \cdot R_{NIP}} \quad [2]$$

In equation [1], we assume that:

$$V_{NMO}^2 = \frac{2V_0 \cdot R_{NIP}}{t_0 \cdot \cos^2\alpha} \quad [3]$$

By inputting equation [3] into equation [2], we will obtain dynamic correction formula:

$$t_{CMP}^2(h) = t_0^2 + \frac{4h^2}{V_{NMO}^2} \quad [4]$$

By analyzing the normal velocity in common middle record section, we can determine stacking velocity $[V_{NMO}]$.

In the next step, the CRS stacking operator is intersected with zero offset section $[h=0]$ and 2D operator [equation 1] is converted into the one-dimensional mode:

$$t_{ZO}^2(x_m) = \left[t_0 + \frac{2\sin\alpha}{V_0} (x_m - x_0) \right]^2 + \frac{2t_0 \cdot \cos^2\alpha}{V_0 \cdot R_N} \cdot [x_m - x_0]^2 \quad [5]$$

In the above equation, parameters α and R_N are unknown. We first assume that a plate wave front has contacted the ground surface:

Research Article

In this case, $R_N = \infty$ and equation [5] is simplified as follows:

$$t_{ZO}(x_m) = t_0 + \frac{2\sin\alpha}{V_0} [x_m - x_0] \quad [6]$$

From this equation, we can obtain the angle of contact between wave and ground surface [α]. Using the value of α and V_{NMO} in equation [3], R_{NIP} is computed.

Likewise, R_N in equation [5] can be determined using the value of α (McClay, 2003; Mitra, 2003; McQuarrie, 2004).

Given that three CRS indicators have been identified for each sample [t_0, x_0], we can add up the data in line with 2D stacking operator [equation 1] in order to obtain CRS stacking section.

To determine optimal parameters, we have to analyze the coherency to select the operator with the highest conformity to real phenomena (Sherkati and Letouzey, 2004).

Structural Situation of the Area under Study

Pazanan anticline is located in Zagros fold and thrust belt, at embayment area of the northern Khuzestan. Researchers have divided Zagros fold and thrust belt into different parts (Abdollahie Fard *et al.*, 2006; Aghanabati, 2006). The majority of the main thrusts of Zagros are located between Iranian and Arabic plates. From northwest to southeast, Zagros fold and thrust belt has been divided into geological states of Lorestan, embayment of the northern Khuzestan, and Fars (Abdollahie Fard *et al.*, 2011). The structural phenomenon of embayment area of the northern Khuzestan is located in the southwest of thrusts and is part of the folded Zagros, in which Asmari formation is not visible. The embayment is situated between three important structural phenomena of the Balarood bending area [left], mountain front bending area, and Kazeroon bending-fault area [right].

The concurrent function of Qatar-Kazeroon lineament [right] and Balarood lineament [left] has played a major role in the formation of this embayment. This region has an area of 3,000-6,000 m, is tectonically more stable than the neighboring regions, and has undergone less folds (Morley, 1988). Pazanan anticline is located in the southeast of Aghajari anticline, northeast of Rageh Sefid anticline, northwest of Bibi Hakimieh and Kheyr Abad anticlines, and southwest of Behbahan and Mansoor Abod anticlines. Geometrical evidences indicate that this structure is a symmetrical anticline with a large and reverse fault in the southern ridge, which is likely to be the continuation of the southern ridge fault of Aghajari anticline. Hendijan anticline with northeast-southwest trend passes through the northwestern part of Pazanan anticline.

Sarook formation map with cenomanian–turonian age indicates the erosion and lack of sedimentation in Hendijan anticline during turonian age. Sarook formation thins at the top of Hendijan anticline. In addition to several deformations which are fully obvious, this formation shows magma activities in the form of volcanic rocks and granite masses. In this study, we aimed to identify the buried faults in the northern plain of Khuzestan using seismic-reflection data. In many cases, earthquake records in the region do not match any of the identified active faults. This may be explained by the fact that few stations exist in the region or the earthquake-causing faults are not visible in the surface and is buried under the sediments. Provided that the stations provide a good coverage, it is essential to study the buried faults of the region [Figure 1].

Data and Analysis Method

The data used in this study includes two-dimensional seismic data in the studied region, geological maps of the northern Khuzestan [1:100000], and SRTM digital images. The seismic-reflection data has been obtained from various resources, including international seismology center [ISC], national Iranian bandwidth seismography network, and geophysics institute of the University of Tehran. The data used in the present study are: two-dimensional seismic-reflection data [University of Tehran], national and international quakes catalogue, and geological data.

We first prepared the map of the existing faults by interpreting the two-dimensional seismic-reflection data. Then, we studied the seismic data obtained from the catalogue of international institute for earthquake engineering and seismology [IIEES] which is a combination of several international catalogues including BS, SSK, RD, ISS, SVE, NA, MOS, STR, USCGS, BCIS, ZEM and SHL [before 1964], the catalogues of USCGS, ISC, IGS, USERL, USGS, IDC and NEIC [1964-2014], and the catalogue of bandwidth seismographic network of IIEES [for the recent years].

Research Article

We first processed the two-dimensional seismography data of the studied region and prepared stacking cross-sections. The data were processed by a processing software. After interpreting the data, we identified some faults in seismography sections. Next, we uploaded the geological map of the region in ARC GIS software and located the processed two-dimensional seismography lines on the same map using their coordinates. Then, we uploaded the recorded earthquakes' data obtained from the catalogue of Iran International Institute of Earthquake Engineering and Seismology onto the map. Next, we interpreted the seismic cross-sections using SRMT. For this purpose, we defined three horizons. After determining the horizons, we determined the fault zones in the seismic lines based on the boundaries of the horizons.

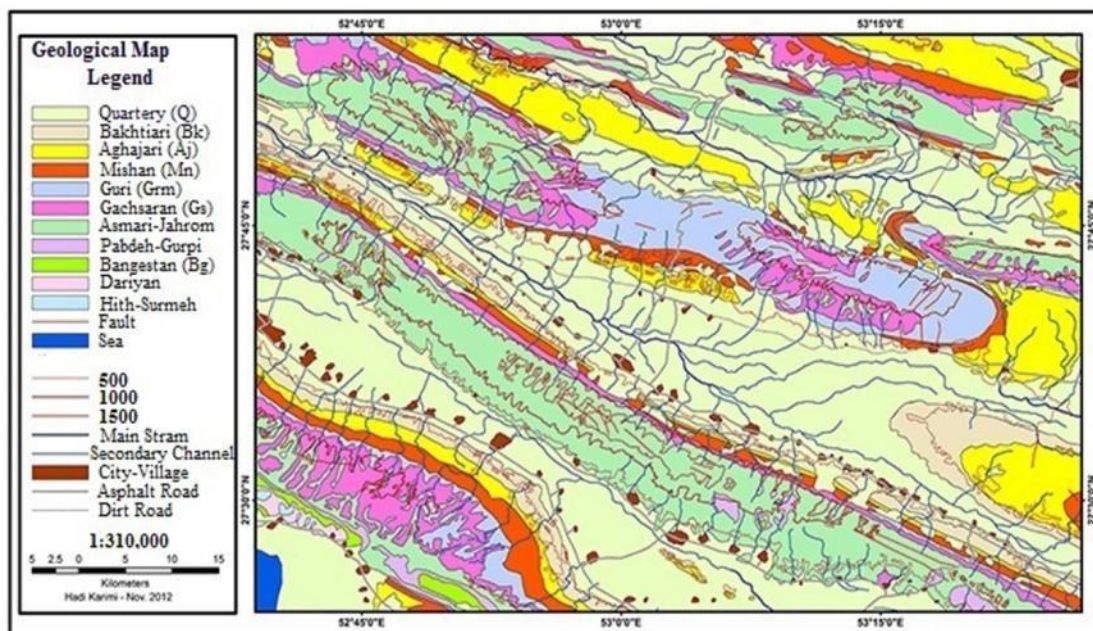


Figure 1: The Region under Study [www.ngdir.ir]

RESULTS AND DISCUSSION

Results

We interpreted the seismic cross-sections using the seismic indicators, but it failed to produce satisfactory results due to bad quality of the data. Then, we studied the geological maps of the northern Khuzestan [1:100000]. The maps did not provide sufficient information due to the alluvial cover of the studied region. In the next step, we studied the earthquakes of the region, which had been obtained from International Seismology Center [ISC], national Iranian bandwidth seismography network, and Geophysics Institute of the University of Tehran [Figure 2].

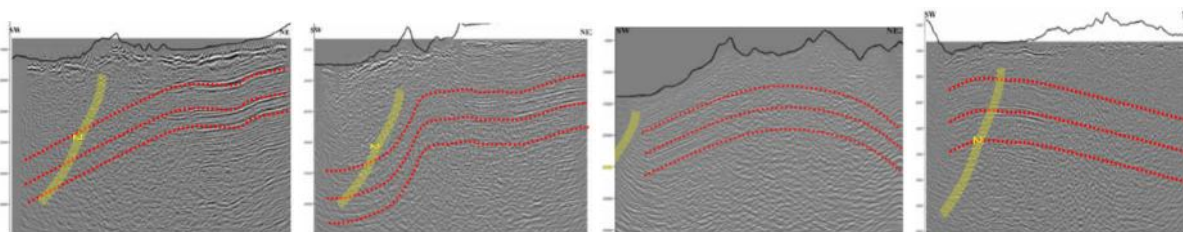
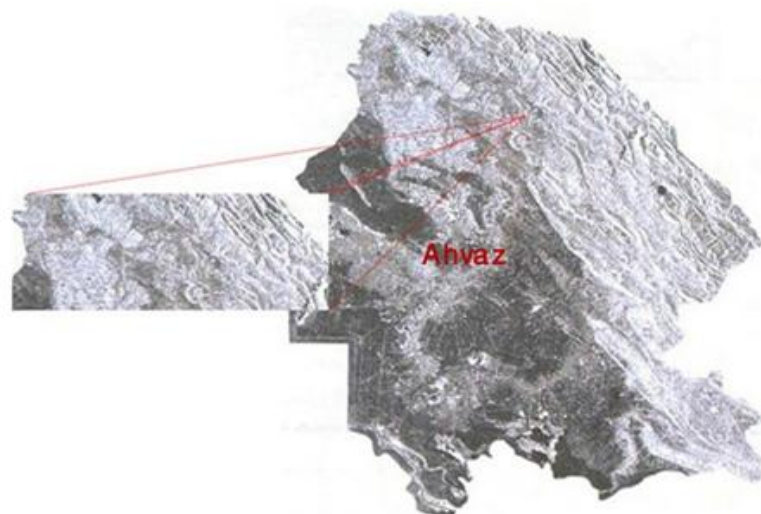
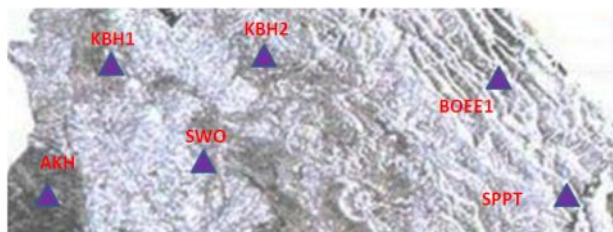


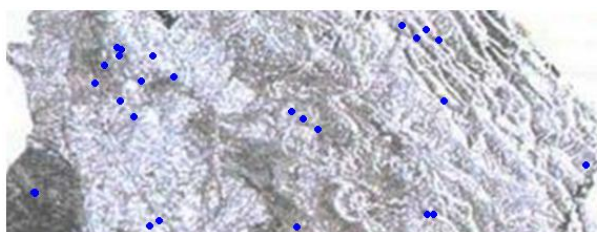
Figure 2: 2D Seismic Cross-Sections for the Northern Khuzestan; These Cross-Sections have NE-SW Trend. The Interpretations Indicate the Presence of many Faults in the Northeast of the Region; Fault [2] [Yellow Color] is Likely to be the Continuation of Fault IRQ168 which has not been Specified due to the Alluvial Cover of the Region; There are Four Horizons in the Cross-Sections



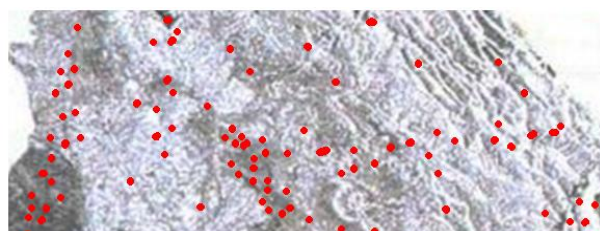
The Region under Study



Quakes Recorded by Seismography Stations [a]



IIEES – Quakes Recorded by Stations [b]



IRSC – Quakes Recorded by Stations [c]



ISC Site [d]



Identified Faults of the Seismic-Reflection Data [e]



Numbers of the Regions [f]

Figure 3: Situation of the Studied Region [1964-2014]

The comparison of the faults with these earthquakes failed to obviously indicate the seismicity of the identified fault, because the majority of earthquakes in the region had a low magnitude and no central mechanism had been determined for them. However, there is an earthquake with the magnitude of $M=2.7$ in the vicinity of fault no. 2 [region no. 1], which was reported by the sites of the Research Institute and Geophysics Institute of the University of Tehran. Moreover, there are two earthquakes in two sides of the fault [3] [regions 2 and 3] and two earthquakes in the vicinity of faults [4] and [5] [regions 4 and 5].

Research Article

These faults are likely to have caused the aforementioned earthquakes. Topographic studies indicated that SW-NE trending lineaments existed in the region. These lineaments are likely to have caused the disruption of NW-SE trending faults in the region. Fault [2] has moved from IRQ168 fault and fault [5]. Earthquakes 4 and 5 are likely to have developed as the result of this contact and separation [Figure 3].

According to figure 3, the numbered earthquakes are likely to be associated with the identified faults. The dotted line is the lineament which is likely to have caused the movement of fault [4] from fault [5] and the movement of fault [2] from the fault IRQ168.

Conclusion

This paper aimed to identify the buried faults in the embayment area of the northern Khuzestan using seismic-reflection data. The studied region is located in the southwest of central Iran, in the vicinity of Uromia Dokhtar region.

Investigation of geological maps indicated that the region did not have any visible faults due to the thick alluvial cover. Interpretation of reflection data and its comparison with the simulated empirical models indicated that many faults existed in the region. The majority of the identified faults had a reverse mechanism with SW slope [faults 1-2]. A number of faults had normal mechanism with NE slope [faults 3-5]. The identified fault [2], located along fault IRQ168, may be the extension of this fault which has been disrupted by SW-NE lineament. This lineament is likely to have caused the movement of fault [3] from fault [1], so these two faults are likely to be a single one.

Investigation of the data indicated that a broken fault zone existed in the north of the region, which consisted of several parallel faults. Mozdooran fault is the main branch of this group and has cut the lines. Further, several smaller faults can be seen in seismic-reflection data, which need to be investigated in the future. The most considerable point is that this group of faults has been identified using seismic-reflection data.

As mentioned earlier, the study of geological maps did not produce satisfactory results. Given the thick alluvial cover, these maps do not show any identified faults in the region. So, the results obtained from the seismic data are the most accurate information on the geological structures of the region. The faults have been introduced for the first time and play a significant role in the determination of seismicity, because they may give rise to several earthquakes in the region.

REFERENCES

- Abdollahie Fard I, Alavi SA and Mokhtari M (2006).** Structural framework of the Abadan plain (SW Iran) and the North Persian Gulf based on the geophysical data. *Iranian International Journal of Science* **32** 107- 121.
- Abdollahie Fard I, Braathen A, Mokhtari M and Alavi SA (2006).** Interaction of the Zagros Fold-thrust belt and the Arabian type, deep-seated folds in the Abadan Plain and the Dezful Embayment, SW Iran. *Petroleum Geoscience* **12** 347–62.
- Abdollahie Fard I, Sepehr M and Sherkati S (2011).** Neogene salt in SW Iran and its interaction with Zagros folding. *Geological Magazine* **148** 854-867.
- Aghanabati A (2006).** *Geology of Iran*. (State Organization of Geology and Mineral Exploration, Tehran) 586.
- Berberian M (1995).** Master-blind-thrust faults hidden under the Zagros folds: Active basement tectonics and surface morphotectonics. *Tectonophysics* **241**(3) 193-224.
- Berberian M and King GCP (1981).** Towards a paleogeography and tectonic evolution of Iran. *Canadian Journal of Earth Sciences* **18** 210-265.
- Blanc EJP, Allen MB, Inger S and Hassani H (2003).** Structural style in the Zagros simple folded zone, Iran. *Journal of Geology Society London* **160** 401-412.
- Colman Sad SP (1978).** Fold development in Zagros simply folded belt, Southwest Iran. *American Association of Petroleum Geologists Bulletin* **62** 984-1003.
- Dahlstrom CDA (1990).** Geometric constraints derived from the law of conservation of volume and applied to evolutionary models for detachment folding. *American Association of Petroleum Geologists Bulletin* **74** 336- 344.

Research Article

- Falcon NL (1969).** Problems of the relationship between surface structures and deep displacements illustrated by the Zagros Range. In: P. Kent, edited by Satterthwaite G.E and Spencer A.M, *Time and Place Orogeny*, (Geological Society of London, Special Publication) 9-22.
- Mann J, Duveneck E, Hertweck T and Jager C (2003).** A seismic reflection imaging workflow based on the Common-Reflection- Surface stack, Technical Report.
- Mann J, Jager R, Muler T, Hocht G and Hubral P (1999).** Common-reflection-surface stack. *Journal of Applied Geophysics* **42** 301-318.
- McClay KR (2003).** Structural Geology for Petroleum Exploration. *Lecture Note* 503.
- McQuarrie N (2004).** Crustal Scale geometry of the Zagros fold-thrust belt, Iran. *Journal of Structural Geology* **26** 519-533.
- Mitra S (2002).** Structural models of faulted detachment folds. *American Association of Petroleum Geologist Bulletin* **86** 1673-1694.
- Mitra S (2003).** A united kinematic model for the evolution of detachment folds. *Journal of Structural Geology* **25** 1659-1673.
- Molinario M, Leturmy P, Guezou JC, Frizon de lamotte D and Eshraghi SA (2005).** The structure and kinematics of the southeastern Zagros fold – thrust belt, Iran: from thin – skinned to thick – skinned tectonics. *Tectonics* **24** 42-60.
- Morley CK (1988).** Out-of-sequence thrusts. *Tectonics* **7** 539-561.
- Motiei H (1993).** *Zagros Stratigraphy*, (Geological Survey of Iran, Tehran, Iran) 536.
- Motiei H (1995).** *Zagros Oil Geology*. State Geology Organization, **1** 589.
- Poblet J and McClay KR (1996).** Geometry and kinematics of single-layer detachment folds. *American Association of Petroleum Geologists Bulletin* **80** 1085-1109.
- Shepherd MF (1963).** Possible Cretaceous trends in the Dezful Embayment. National Iranian Oil Company. Technical Memo, **14**, Unpublished Report.
- Sherkati S and Letouzey J (2004).** Variation of structural style and basin evolution in the central Zagros (Izeh Zone and Dezful Embayment), Iran. *Marine and Petroleum Geology* **21** 535-554.
- Stocklin J (1968).** Salt deposits of the Middle East. *Geological of Society America- Special Paper* **88** 157- 181.
- Stoneley R (1981).** The geology of the Kuh-e-Dalneshin area of Southern Iran, and its bearing on the evolution of southern Tethys. *Journal of Geological Society of London* **138** 509-526.
- Tatar M, Hatzfeld D, Martinod J, Walpersdorf A, Ghafari – Ashtiany M and Chery J (2002).** The present day deformation of the central Zagros from GPS measurements. *Geophysics* **29** 1-4.
- Tygel M, Muller T, Hubral P and Schleicher J (1997).** Eigen wave based multi parameter travel time expansions. *67th Annual International Meeting: Society of Exploration Geophysicists. Expanded Abstract* 1770-1773.
- Vita-Finzi C (2001).** Neotectonics at the Arabian plate margins. *Journal of Structural Geology* **23** 521-530.